

UV Resonance Raman Determination of Polyproline II, Extended 2.5₁-Helix, and β -Sheet Ψ Angle Energy Landscape in Poly-L-Lysine and Poly-L-Glutamic Acid

Aleksandr V. Mikhonin, Nataliya S. Myshakina, Sergei V. Bykov, and Sanford A. Asher*

Contribution from the Department of Chemistry, University of Pittsburgh, Pittsburgh, Pennsylvania 15260

Received September 3, 2004; E-mail: asher@pitt.edu

Abstract: UV resonance Raman (UVR) spectroscopy was used to examine the solution conformation of poly-L-lysine (PLL) and poly-L-glutamic acid (PGA) in their non- α -helical states. UVR measurements indicate that PLL (at pH = 2) and PGA (at pH = 9) exist mainly in a mixture of polyproline II (PPII) and a novel left-handed 2.5₁-helical conformation, which is an extended β -strand-like conformation with $\Psi \approx +170^\circ$ and $\Phi \approx -130^\circ$. Both of these conformations are highly exposed to water. The energies of these conformations are very similar. We see no evidence of any disordered "random coil" states. In addition, we find that a PLL and PGA mixture at neutral pH is $\sim 60\%$ β -sheet and contains PPII and extended 2.5₁-helix conformations. The β -sheet conformation shows little evidence of amide backbone hydrogen bonding to water. We also developed a method to estimate the distribution of Ψ Ramachandran angles for these conformations, which we used to estimate a Ψ Ramachandran angle energy landscape. We believe that these are the first experimental studies to give direct information on protein and peptide energy landscapes.

Introduction

The primary sequence of a protein encodes both the native structure as well its folding mechanism^{1–8} (in the absence of chaperones or post-translational modifications). Arguably, the most important problem in enzymology is to translate the protein primary sequence into the encoded protein folding mechanism(s) and to use this information to predict the ultimate native structure from the primary sequence information. In general, the native conformation(s) are thought to be located at distinct minima in the potential energy landscape.^{9–15} The native conformation occurs when the protein environment favors folding.^{16–20}

Until recently, protein unfolded states were assumed to consist of random coil conformations, where the polypeptide chains would adopt energetically allowed but randomly distributed Φ and Ψ dihedral angles. Ideally, these structures were considered to be completely disordered with no correlations between adjacent peptide bonds Φ and Ψ Ramachandran dihedral angles.²¹ However, this assumption has recently been seriously challenged.^{22–28}

Numerous theoretical and experimental groups have been working on elucidating protein folding mechanisms over the last 50 years.^{1–21,23–28} A major challenge in this work is the required development of an energetic understanding of protein folding motifs and the sequence-specific phenomena that determine the folding energy landscape. In this regard, new theoretical paradigms such as the energy landscape theories have significantly aided thinking about protein folding. In addition, new theoretical studies have examined the conformational

- (1) Creighton, T. E. *Protein Folding*; W. H. Freeman: New York, 1992.
- (2) Baldwin, R. L. *Nature* **1990**, *346*, 409–410.
- (3) Kim, P. S.; Baldwin, R. L. *Annu. Rev. Biochem.* **1990**, *59*, 631–660.
- (4) Matthews, C. R. *Annu. Rev. Biochem.* **1993**, *62*, 653–683.
- (5) Fernandez-Carneado, J.; Grell, D.; Durieux, P.; Hauert, J.; Kovacsovic, T.; Tuchscherer, G. *Biopolymers* **2000**, *55*, 451–458.
- (6) Bryngelson, J. D.; Onuchic, J. N.; Socci, N. D.; Wolynes, P. G. *Proteins: Struct., Funct., Genet.* **1995**, *21*, 167–195.
- (7) Thirumalai, D.; Woodson, S. A. *Acc. Chem. Res.* **1996**, *29*, 433–439.
- (8) Pennisi, E. *Science* **1996**, *273*, 426–428.
- (9) Chan, H. S.; Dill, K. A. *Proteins: Struct., Funct., Genet.* **1998**, *30*, 2–33.
- (10) Dill, K. A. *Biochemistry* **1990**, *29*, 7133–7155.
- (11) Pokarowski, P.; Kolinski, A.; Skolnick, J. *Biophys. J.* **2003**, *84*, 1518–1526.
- (12) Jewett, A. I.; Pande, V. S.; Plaxco, K. W. *J. Mol. Biol.* **2003**, *326*, 247–253.
- (13) Hardin, C.; Eastwood, M. P.; Prentiss, M.; Luthey-Schulten, Z.; Wolynes, P. G. *J. Comput. Chem.* **2002**, *23*, 138–146.
- (14) Alm, E.; Baker, D. *Proc. Natl. Acad. Sci. U.S.A.* **1999**, *96*, 11305–11310.
- (15) Socci, N. D.; Onuchic, J. N.; Wolynes, P. G. *Proteins: Struct., Funct., Genet.* **1998**, *32*, 136–158.
- (16) Anfinsen, C. B. *Science* **1973**, *181*, 223–230.
- (17) Mayor, U.; Guydosh, N. R.; Johnson, C. M.; Grossmann, J. G.; Sato, S.; Jas, G. S.; Freund, S. M. V.; Alonso, D. O. V.; Daggett, V.; Fersht, A. R. *Nature* **2003**, *421*, 863–867.
- (18) Myers, J. K.; Oas, T. G. *Annu. Rev. Biochem.* **2002**, *71*, 783–815.

- (19) Mirny, L.; Shakhnovich, E. *Annu. Rev. Biophys. Biomol. Struct.* **2001**, *30*, 361–396.
- (20) Englander, S. W. *Annu. Rev. Biophys. Biomol. Struct.* **2000**, *29*, 213–238, 213 Plates.
- (21) Flory, P. J. *Statistical Mechanics of Chain Molecules*; Interscience: New York, 1969.
- (22) Tiffany, M. L.; Krimm, S. *Biopolymers* **1968**, *6*, 1379–1382.
- (23) Pappu, R. V.; Srinivasan, R.; Rose, G. D. *Proc. Natl. Acad. Sci. U.S.A.* **2000**, *97*, 12565–12570.
- (24) Srinivasan, R.; Rose, G. D. *Proc. Natl. Acad. Sci. U.S.A.* **1999**, *96*, 14258–14263.
- (25) Marqusee, S.; Robbins, V. H.; Baldwin, R. L. *Proc. Natl. Acad. Sci. U.S.A.* **1989**, *86*, 5286–5290.
- (26) Pal, D.; Suhnel, J.; Weiss, M. S. *Angew. Chem., Int. Ed.* **2002**, *41*, 4663–4665.
- (27) Watson, J. D.; Milner-White, E. J. *J. Mol. Biol.* **2002**, *315*, 183–191.
- (28) Watson, J. D.; Milner-White, E. J. *J. Mol. Biol.* **2002**, *315*, 171–182.

subspace of small and large peptides and have examined conformational energies. Molecular dynamical studies are becoming available which examine the temporal evolution of protein structure in time scales that are relevant for folding into equilibrium structures.^{29–33}

This work has been aided by new experimental studies that characterize peptide conformations.^{34–49} What is most needed to continue progress is additional experimental insight into protein folding motifs and the energy mountain ranges that surround these structures.

We,^{50–52} as well as others,^{53–58} have been developing UV Raman spectroscopy (UVRS) to probe protein structure and dynamics. We recently examined the first stages in unfolding of α -helices and discovered that a mainly ala 21-residue peptide melts from an α -helix conformation into a polyproline II conformation (PPII).³⁴

In this work, we examine peptide conformations of peptides such as poly-L-glutamic acid (PGA) and poly-L-lysine (PLL) under conditions where their side chains are charged. We find that they occur as a mixture of PPII and a novel conformation, which is a subset of extended β -strand conformations, but which is best described as a 2.5₁-helix. If the side chain charges are neutralized, these peptides form α -helices, whereas if peptides with oppositely charged side chains are mixed, they form β -sheet conformations.⁵⁹

We have developed insights into peptide secondary structures through examinations of their \sim 200-nm UV resonance Raman spectra. We obtain the most information from the amide III₃ (AmIII₃)³⁶ vibration whose frequency we earlier found was correlated to the peptide conformational Ramachandran Ψ angle.^{34,60,61} We have recently developed quantitative relationships between peptide bond AmIII₃ frequencies, the peptide bond Ψ angle, and its hydrogen bonding pattern.⁶¹ In this work, these relationships are used to estimate the conformational energy differences between the PPII and 2.5₁-helix conformations, the Ψ angle energy landscape for the PPII and 2.5₁-helix conformations, as well as for the β -sheet structure. To our knowledge, these are the first experimental studies to directly give information on the energy landscape of peptide conformations along coordinates involved in conformational evolution.

This work shows clearly that the UVRS spectra of β -sheet conformations significantly differ from those of PPII and 2.5₁-helix (“single” β -strand) conformations. This ability to discriminate between conformations may prove useful for early detection of amyloid fibril formation in solutions of proteins.⁶²

Experimental Section

Sample Preparation. Poly-L-Lysine HCl (PLL, MW_{vis} = 28 500, MW_{LALLS} = 20 200) and the sodium salt of poly-L-glutamic acid (PGA, MW_{vis} = 17 000, MW_{MALLS} = 8853) were purchased from Sigma Chemical and used as received. Solution spectra of PLL and PGA were measured at pH = 2 and pH = 9, respectively, to ensure the absence of α -helix contributions. The mixed PLL and PGA neutral pH sample solutions contained identical concentrations of lysine and glutamic acid residues. These samples were freshly prepared before the Raman measurements. The total peptide concentrations were kept below 0.3 mg/mL to avoid gel formation.

The 21-residue alanine-based peptide AAAAA(AAARA)₃A (AP) was prepared (HPLC pure) at the Pittsburgh Peptide Facility by using the solid-state peptide synthesis method. The AP solutions in water contained 1 mg/mL concentrations of AP and 0.2 M concentrations of sodium perchlorate, which was used as an internal intensity and frequency standard. All Raman spectra were normalized to the intensity of the ClO₄⁻ Raman band (932 cm⁻¹).

A₅ and A₃ peptides were purchased from Bachem Bioscience, Inc. (King of Prussia, PA) and used as received. The A₅ – A₃ Raman difference spectral measurements utilized identical molar concentrations of A₅ and A₃ (0.34 and 0.2 mg/mL, respectively) in solutions containing identical sodium perchlorate concentrations (0.2 M). We normalized the Raman spectra to the intensity of the 932 cm⁻¹ perchlorate internal standard band. The A₅ – A₃ difference spectra were calculated by subtracting the normalized A₃ spectrum from the normalized A₅ spectrum at each temperature.

The undecapeptide XAO (MW = 985) was prepared (HPLC pure) at the Pittsburgh Peptide Facility by using the solid-state peptide synthesis method. The sequence of this peptide is Ac-XXAAAAAAOO-amide, where all amino acids are in their L form, A is ala, X is diaminobutyric acid (side chain CH₂CH₂NH₃⁺), and O is ornithine (side chain (CH₂)₃NH₃⁺). We used 1 mg/mL solutions of XAO peptide containing 0.15 M sodium perchlorate. The UVRR spectra of XAO were also normalized to the ClO₄⁻ Raman band intensity.

- (29) Sreerama, N.; Woody, R. W. *Proteins: Struct., Funct., Genet.* **1999**, *36*, 400–406.
 (30) Park, C.; Carlson, M. J.; Goddard, W. A. I. *J. Phys. Chem. A* **2000**, *104*, 2498–2503.
 (31) Wu, X.; Wang, S. *J. Phys. Chem. B* **2001**, *105*, 2227–2235.
 (32) Wiczorek, R.; Dannenberg, J. J. *J. Am. Chem. Soc.* **2003**, *125*, 8124–8129.
 (33) Avbelj, F.; Fele, L. *J. Mol. Biol.* **1998**, *279*, 665–684.
 (34) Asher, S. A.; Mikhonin, A. V.; Bykov, S. B. *J. Am. Chem. Soc.* **2004**, *126*, 8433–8440.
 (35) Shi, Z.; Olson, C. A.; Rose, G. D.; Baldwin, R. L.; Kallenbach, N. R. *Proc. Natl. Acad. Sci. U.S.A.* **2002**, *99*, 9190–9195.
 (36) Mikhonin, A. V.; Ahmed, Z.; Ianoul, A.; Asher, S. A. *J. Phys. Chem. B* **2004**, *108*, 19020–19028.
 (37) Mikhonin, A. V.; Asher, S. A. *J. Phys. Chem. B* **2005**, *109*, 3047–3052.
 (38) Woutersen, S.; Hamm, P. *J. Chem. Phys.* **2001**, *114*, 2727–2737.
 (39) Eker, F.; Cao, X.; Nafie, L.; Schweitzer-Stenner, R. *J. Am. Chem. Soc.* **2002**, *124*, 14330–14341.
 (40) Fang, C.; Wang, J.; Charnley, A. K.; Barber-Armstrong, W.; Smith, A. B.; Decatur, S. M.; Hochstrasser, R. M. *Chem. Phys. Lett.* **2003**, *382*, 586–592.
 (41) Fang, C.; Wang, J.; Kim, Y. S.; Charnley, A. K.; Barber-Armstrong, W.; Smith, A. B., III; Decatur, S. M.; Hochstrasser, R. M. *J. Phys. Chem. B* **2004**, *108*, 10415–10427.
 (42) Eker, F.; Griebenow, K.; Cao, X.; Nafie, L. A.; Schweitzer-Stenner, R. *Biochemistry* **2004**, *43*, 613–621.
 (43) Demirdoeven, N.; Cheatum, C. M.; Chung, H. S.; Khalil, M.; Knoester, J.; Tokmakoff, A. *J. Am. Chem. Soc.* **2004**, *126*, 7981–7990.
 (44) Hamm, P.; Lim, M.; DeGrado, W. F.; Hochstrasser, R. M. *Proc. Natl. Acad. Sci. U.S.A.* **1999**, *96*, 2036–2041.
 (45) Kocak, A.; Luque, R.; Diem, M. *Biopolymers* **1998**, *46*, 455–463.
 (46) Woutersen, S.; Hamm, P. *J. Phys.: Condens. Matter* **2002**, *14*, R1035–R1062.
 (47) Woutersen, S.; Hamm, P. *J. Chem. Phys.* **2001**, *115*, 7737–7743.
 (48) Eker, F.; Griebenow, K.; Cao, X.; Nafie, L. A.; Schweitzer-Stenner, R. *Proc. Natl. Acad. Sci. U.S.A.* **2004**, *101*, 10054–10059.
 (49) Pimenov, K. V.; Bykov, S. V.; Mikhonin, A. V.; Asher, S. A. *J. Am. Chem. Soc.* **2005**, *127*, 2840–2841.
 (50) Asher, S. A. In *Handbook of Vibrational Spectroscopy*; Chalmers, J. M., Griffiths, P. R., Eds.; Wiley & Sons: New York, 2001; Vol. 1, pp 557–571.
 (51) Lednev, I. K.; Karnoup, A. S.; Sparrow, M. C.; Asher, S. A. *J. Am. Chem. Soc.* **1999**, *121*, 8074–8086.
 (52) Chi, Z.; Chen, X. G.; Holtz, J. S. W.; Asher, S. A. *Biochemistry* **1998**, *37*, 2854–2864.
 (53) Wen, Z. Q.; Thomas, G. J., Jr. *Biochemistry* **2000**, *39*, 146–152.
 (54) Wang, D.; Zhao, X.; Shen, T.-J.; Ho, C.; Spiro, T. G. *J. Am. Chem. Soc.* **1999**, *121*, 11197–11203.
 (55) Kim, J. E.; Pan, D.; Mathies, R. A. *Biochemistry* **2003**, *42*, 5169–5175.
 (56) Serban, D.; Arcineiga, S. F.; Vorgias, C. E.; Thomas, G. J., Jr. *Protein Sci.* **2003**, *12*, 861–870.
 (57) Haruta, N.; Kitagawa, T. *Biochemistry* **2002**, *41*, 6595–6604.
 (58) Thomas, G. J., Jr. *Annu. Rev. Biophys. Biomol. Struct.* **1999**, *28*, 1–27.

- (59) Ismail, A. A.; Mantsch, H. H. *Biopolymers* **1992**, *32*, 1181–1186.
 (60) Asher, S. A.; Ianoul, A.; Mix, G.; Boyden, M. N.; Karnoup, A.; Diem, M.; Schweitzer-Stenner, R. *J. Am. Chem. Soc.* **2001**, *123*, 11775–11781.
 (61) Mikhonin, A. V.; Bykov, S. V.; Asher, S. A. *J. Am. Chem. Soc.*, submitted for publication, **2005**.
 (62) Lednev, I. K.; Carlsen, A.; Ermolenkov, V. V.; He, W.; Higashiya, S.; Topilina, N.; Wells, C. C.; Welch, J. T.; Xu, M. *Book of Abstracts*, 31st Annual Meeting of the Federation of Analytical Chemistry and Spectroscopy Societies, Portland, OR, October 3–7, 2004; Federation of Analytical Chemistry and Spectroscopy Societies: Santa Fe, NM, 2004; p 142.

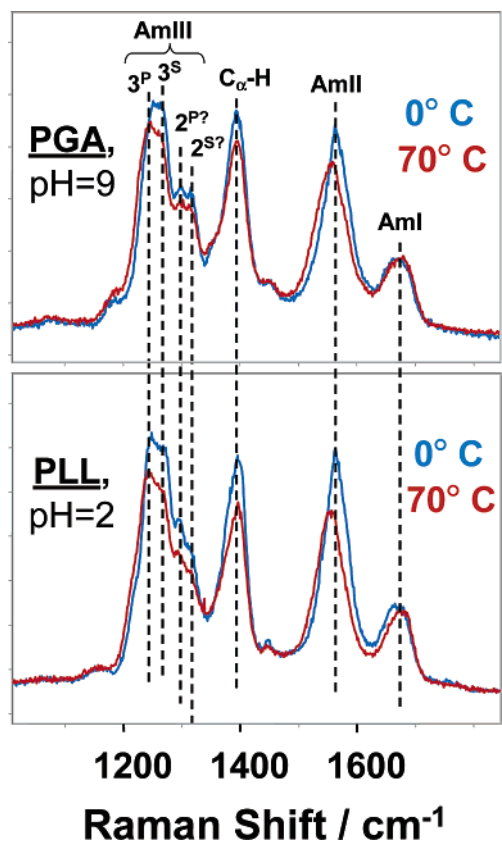


Figure 1. UVR spectra (204 nm) of unfolded states of PGA (pH = 9) and PLL (pH = 2) in water at 0 °C and at +70 °C.

UV Resonance Raman Instrumentation. The Raman instrumentation has been described in detail elsewhere.^{51,63,64} A Coherent Infinity Nd:YAG laser produced 355-nm (3rd harmonic), 3-ns pulses at 100 Hz. This beam was Raman shifted to 204 nm (5th anti-Stokes) by using a 1-m tube filled with hydrogen (60 psi). A Pellin Broca prism was used to select the 204-nm excitation beam. The Raman scattered light was imaged into a subtractive double spectrometer,⁶⁴ and the UV light was detected by a Princeton Instruments solar blind ICCD camera. All samples were measured in a thermostated free surface flow stream.

Results and Discussion

1. Unfolded States of PLL and PGA. Figure 1 shows the 204-nm UV resonance Raman (UVR) spectra of the unfolded conformations of PLL (pH = 2) and PGA (pH = 9) at high (+70 °C) and low (0 °C) temperatures. At these pH values, PLL and PGA have charged side chains whose repulsions prevent formation of α -helical conformations. The UVR spectra of the PLL and PGA samples are essentially identical. Further, the insignificant spectral shifts occurring between the low- and high-temperature spectra indicate a lack of conformational transitions over this temperature range.

The 0 °C spectra show the AmI bands at ~ 1670 cm^{-1} (mainly CO s), the AmII bands at ~ 1564 cm^{-1} (mainly out of phase combination of CN s and NH b), the (C)C α -H bending bands at ~ 1396 cm^{-1} , and a complex series of bands in the AmIII region between 1210 and 1350 cm^{-1} . The AmIII region contains at least four resolved bands, which as discussed below derive from two conformations in equilibrium. We assign these two

conformations to a polyproline II conformation (PPII, P superscript) and an extended β -strand-like conformation (S superscript). As discussed below, the latter conformation can be described as an extended 2.5 $_1$ -helix. As evident from previous UVR studies^{36,37,52,60} the AmIII bands are significantly more sensitive to conformation than are the AmI and AmII bands that are more typically used by IR absorption and normal nonresonance Raman secondary structure studies. Moreover, the UVR AmIII $_3$ band is independently contributed by the individual peptide bonds in the polypeptides with no evidence of interamide coupling,^{37,65} in contrast to the commonly utilized AmI band.^{37,40} These important observations dramatically simplify the spectral analysis in the AmIII region.

Thus, we enumerate these bands as AmIII $_3^S$ (~ 1271 cm^{-1} (PLL) and ~ 1272 cm^{-1} (PGA)), AmIII $_3^P$ (~ 1245 cm^{-1} (PLL) and ~ 1249 cm^{-1} (PGA)), AmIII $_2^{S?}$ (~ 1316 cm^{-1} (PLL) and ~ 1319 cm^{-1} (PGA)), and AmIII $_2^{P?}$ (~ 1296 cm^{-1} (PLL) and ~ 1298 cm^{-1} (PGA)), where the subscripts label different amide III spectral region bands as we recently discussed in detail,³⁶ and the superscript question mark labels assignments that remain uncertain.

The temperature dependence of the spectra involves small downshifts for the AmIII and AmII bands and small upshifts for the AmI band (Table 1) as the temperature increases. This temperature dependence is characteristic of peptide backbone conformations where the amide carbonyl and N-H groups are hydrogen bonded to water.^{34,36,66} The shifts occur because the water-amide hydrogen bond strengths decrease as the temperature increases.³⁴ This favors a peptide bond resonance form with stronger bonding for the carbonyl and weaker bonding for the C(O)-N linkage, which result in the observed amide band shifts.

AmIII $_3^P$ Band (~ 1245 cm^{-1}) Signals PPII Conformations. Figure 2 compares the 204-nm UVR spectra of the unfolded PGA and PLL samples to spectra of the three ala-based peptides: XAO, AP, and A $_5$ -A $_3$ under conditions where they are predominantly in PPII conformations. The observed AmIII $_3^P$ band frequency closely coincides with the AmIII $_3$ frequency of the PPII conformations of XAO, AP, and A $_5$ -A $_3$. Since we know that the AmIII $_3$ frequency strongly depends on the Ψ angle^{34,60} (and to much lesser degree on *allowed* Φ angles^{34,60,67-69}), we conclude that both PLL and PGA have solution conformations with Ψ angles similar to that of the PPII conformation.

The coincidence in frequency and the similar temperature dependencies (Table 1) of the AmIII $_3^P$ bands to those of PPII conformations militates for the assignment of this band to PPII conformations of PGA and PLL. This conclusion is consistent with previous studies that also concluded that the unfolded state(s) of PLL and PGA have significant PPII content.^{22,70-81}

(63) Lednev, I. K.; Kamoup, A. S.; Sparrow, M. C.; Asher, S. A. *J. Am. Chem. Soc.* **2001**, *123*, 2388-2392.

(64) Bykov, S. B.; Lednev, I. K.; Ianoul, A.; Asher, S. A. In preparation, 2005.

(65) Mix, G.; Schweitzer-Stenner, R.; Asher, S. A. *J. Am. Chem. Soc.* **2000**, *122*, 9028-9029.

(66) Torii, H.; Tatsumi, T.; Tasumi, M. *J. Raman Spectrosc.* **1998**, *29*, 537-546.

(67) Ianoul, A.; Boyden, M. N.; Asher, S. A. *J. Am. Chem. Soc.* **2001**, *123*, 7433-7434.

(68) Mirkin, N. G.; Krimm, S. *J. Phys. Chem. A* **2002**, *106*, 3391-3394.

(69) Abbruzzetti, S.; Viappiani, C.; Small, J. R.; Libertini, L. J.; Small, E. W. *J. Am. Chem. Soc.* **2001**, *123*, 6649-6653.

(70) Rucker, A. L.; Creamer, T. P. *Protein Sci.* **2002**, *11*, 980-985.

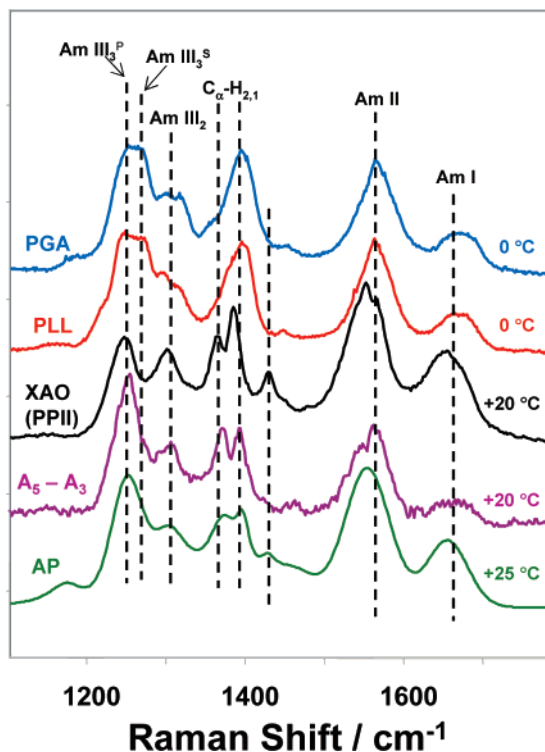
(71) Smyth, E.; Syme, C. D.; Blanch, E. W.; Hecht, L.; Vasak, M.; Barron, L. D. *Biopolymers* **2001**, *58*, 138-151.

(72) Woody, R. W. *Adv. Biophys. Chem.* **1992**, *2*, 37-79.

(73) Keiderling, T. A.; Silva, R. A.; Yoder, G.; Dukor, R. K. *Bioorg. Med. Chem.* **1999**, *7*, 133-141.

Table 1. Temperature Dependence of Amide UV Raman Bands of Non- α -Helical Polypeptides: pH = 2 PLL, pH = 9 PGA, and PPII Peptides: XAO, Ala₅-Ala₃, AP

	XAO-peptide >80% PPII, neutral pH		Ala ₅ -Ala ₃ essentially PPII, neutral pH		AP essentially PPII, neutral pH		PLL unfolded (PPII + extended), pH = 2		PGA unfolded (PPII + extended), pH = 9	
	d ν /dT	$\nu_{60^\circ\text{C}}$, cm ⁻¹	d ν /dT	$\nu_{50^\circ\text{C}}$, cm ⁻¹	d ν /dT	$\nu_{60^\circ\text{C}}$, cm ⁻¹	d ν /dT	$\nu_{70^\circ\text{C}}$, cm ⁻¹	d ν /dT	$\nu_{70^\circ\text{C}}$, cm ⁻¹
AI	0.02 ± 0.01	1659	0.052 ± 0.02	1667	0.052 ± 0.02	1659	0.06	1673	0.03	1673
AII	-0.14 ± 0.01	1545	-0.14 ± 0.01	1558	-0.14 ± 0.01	1548	-0.15	1553	-0.13	1555
C α H ₍₁₎	0.008 ± 0.016	1388	-0.015 ± 0.02	1397	-0.015 ± 0.02	1399	-0.01	1399	0.02	1396
C α H ₍₂₎	0.018 ± 0.017	1365	-0.01 ± 0.02	1373	-0.01 ± 0.03	1377 broad	-0.04	1377	0.036	1359
AIII ₂	-0.03 ± 0.02	1300	-0.03 ± 0.01	1305	-0.03 ± 0.01	1311	-0.033	1313	-0.003	1319
AIII ₃ ^S (2.5 ₁ -helix)	N/A	N/A	N/A	N/A	N/A	N/A	-0.036	1293	-0.006	1298
AIII ₃ ^P (PPII)	-0.10 ± 0.02	1241	-0.094 ± 0.018	1250	-0.094 ± 0.018	1247	-0.1	1242	-0.12	1240

**Figure 2.** Comparison of 204-nm UVR spectra of unfolded states of PGA (pH = 9) and PLL (pH = 2) in water at 0 °C to the spectra of the PPII states of alanine-rich peptides XAO, AP, and A₅-A₃ at 0 °C.

The PPII structure is a commonly observed non- α -helix low-energy conformation because of its stabilization by peptide-water interactions.^{72,82,83} This open conformation permits the simultaneous hydrogen bonding of water to amide bonds, as well as important bridging hydrogen bonds between water molecules. In addition, Hinderaker and Raines⁸⁴ recently

proposed an additional PPII stabilization mechanism. They suggested that the PPII conformation is stabilized because of especially favorable $n-\pi^*$ interactions between the carbonyl oxygen of peptide bonds and the carbonyl carbons of adjacent peptide bonds. Whatever the case, investigators now find that the unfolded states of many proteins^{71,82,85-89} as well as the unfolded states of moderate and long peptides^{35,70-73} and even small peptides⁹⁰⁻⁹² contain significant fractions of PPII.

AmIII₃^S Band (~1271 cm⁻¹) Signals the Presence of a β -Strand (2.5₁-Helix) Conformation. The electrostatic repulsions between the PLL- and PGA-charged side chains prevent formation of α -helical conformations and should force more extended conformations, such as PPII and/or extended β -strand(s). The PPII conformation clearly does not require side chain repulsion since it occurs for polyalanine derivatives such as AP and XAO.^{34,35,93} Further, the K7 peptide shows significant PPII content at pH = 12 in the absence of salt as well as in 4 M NaCl.⁷⁰

The pH = 2 PLL and pH = 9 PGA spectra also show a second AmIII₃ region band at ~1271 cm⁻¹ denoted as AmIII₃^S (Figures 1 and 2). This band is absent in mainly PPII ala-based peptides with neutral side chains. Thus, it must result from the additional PLL and PGA electrostatic repulsions between ionized side chains. We expect that these repulsions will induce a more extended conformation with a Ramachandran angle greater than the $\Psi = 145^\circ$ of the PPII conformation. Given the dependence of the AmIII₃ frequency on the Ψ angle that we previously demonstrated,^{34,36,60} we expect a new AmIII₃ band to occur at a higher frequency, as observed.

Because of the severe overlap with the AmIII₃^P bands, it is not possible to accurately determine the AmIII₃^S temperature dependence. However, the temperature dependence is qualitatively similar to that of fully exposed conformations such as PPII. Thus, we assign the conformation to an extended β -strand-like conformation (2.5₁-helix, see below) and conclude that these

(74) Drake, A. F.; Siligardi, G.; Gibbons, W. A. *Biophys. Chem.* **1988**, *31*, 143-146.
 (75) Wilson, G.; Hecht, L.; Barron, L. D. *J. Chem. Soc., Faraday Trans.* **1996**, *92*, 1503-1509.
 (76) Yasui, S. C.; Keiderling, T. A. *J. Am. Chem. Soc.* **1986**, *108*, 5576-5581.
 (77) Birke, S. S.; Agbaje, I.; Diem, M. *Biochemistry* **1992**, *31*, 450-455.
 (78) Paterlini, M. G.; Freedman, T. B.; Nafie, L. A. *Biopolymers* **1986**, *25*, 1751-1765.
 (79) Dukor, R. K.; Keiderling, T. A. *Biopolymers* **1991**, *31*, 1747-1761.
 (80) Dukor, R. K.; Keiderling, T. A. *Pept., Proc. Eur. Pept. Symp., 20th* **1989**, 519-521.
 (81) Dukor, R. K.; Keiderling, T. A. *Gut, V. Int. J. Pept. Protein Res.* **1991**, *38*, 198-203.
 (82) Bochicchio, B.; Tamburro, A. M. *Chirality* **2002**, *14*, 782-792.
 (83) Mezei, M.; Fleming, P. J.; Srinivasan, R.; Rose, G. D. *Proteins: Struct., Funct., Bioinf.* **2004**, *55*, 502-507.
 (84) Hinderaker, M. P.; Raines, R. T. *Protein Sci.* **2003**, *12*, 1188-1194.

(85) Shi, Z.; Woody, R. W.; Kallenbach, N. R. *Adv. Prot. Chem.* **2002**, *62*, 163-240.
 (86) Adzhubei, A. A.; Sternberg, M. J. E. *J. Mol. Biol.* **1993**, *229*, 472-493.
 (87) Syme, C. D.; Blanch, E. W.; Holt, C.; Jakes, R.; Goedert, M.; Hecht, L.; Barron, L. D. *Eur. J. Biochem.* **2002**, *269*, 148-156.
 (88) Sreerama, N.; Woody, R. W. *Biochemistry* **1994**, *33*, 10022-10025.
 (89) Cao, W.; Bracken, C.; Kallenbach, N. R.; Lu, M. *Protein Sci.* **2004**, *13*, 177-189.
 (90) Gnanakaran, S.; Hochstrasser, R. M. *J. Am. Chem. Soc.* **2001**, *123*, 12886-12898.
 (91) Woutersen, S.; Hamm, P. *J. Phys. Chem. B* **2000**, *104*, 11316-11320.
 (92) Schweitzer-Stenner, R.; Eker, F.; Huang, Q.; Griebenow, K.; Mroz, P. A.; Kozlowski, P. M. *J. Phys. Chem. B* **2002**, *106*, 4294-4304.
 (93) McColl, I. H.; Blanch, E. W.; Hecht, L.; Kallenbach, N. R.; Barron, L. D. *J. Am. Chem. Soc.* **2004**, *126*, 5076-5077.

Table 2. Temperature Dependencies of Amide UV Raman Bands of PLL–PGA Mixture

	PLL–PGA mixture, ~60% β -sheet, ~40% unfolded, ^a neutral pH		PLL–PGA mixture, pure PPII, 2.5 ₁ conformations ^b neutral pH		PLL–PGA mixture, pure β -sheet spectrum ^b neutral pH	
	d ν /dT	$\nu_{70^\circ\text{C}}$, cm ⁻¹	d ν /dT	$\nu_{70^\circ\text{C}}$, cm ⁻¹	d ν /dT	$\nu_{70^\circ\text{C}}$, cm ⁻¹
AI	0.022	1668	0.045		0.018	1672
AII	-0.071	1548	-0.14		-0.005	1550
C α H ₍₁₎	-0.007	1402	0.005		-0.031	1403
C α H ₍₂₎	0	1381	-0.005		0	1379 weak
AmI ₂	0	1290	-0.03			
		1310				
AmI ₃	-0.062	1239	-0.11		-0.003	1228

^a Experimental spectra, neutral pH (~50% β -sheet, ~50% unfolded). ^b See text for details.

Table 3. Distances between Ionized Side Chain Charges in PLL and PGA for Ψ and Φ Angles of PPII and 2.5₁-Helix Conformations

	distance between side chain charges	PPII	extended 2.5 ₁ -helix
		$\Psi = +145^\circ$ $\Phi = -75^\circ$	$\Psi = +170^\circ$ $\Phi = -130^\circ$
PLL	$i \rightarrow i+1$	11.245	11.67
	$i \rightarrow i+2$	12.389	10.146
	$i \rightarrow i+3$	9.232	12.266
	$i \rightarrow i+4$	16.427	18.130
PGA	$i \rightarrow i+1$	8.328	8.421
	$i \rightarrow i+2$	9.852	8.639
	$i \rightarrow i+3$	9.232	11.381
	$i \rightarrow i+4$	14.563	16.101

Table 4. Ψ Angle Distribution of PPII Helix, 2.5₁-Helix, and β -Sheet Conformations of PLL and PGA^a

conformation	σ , deg	R = 2.5 ₁ -helix/ PPII-helix	$\Delta G = G(\text{PPII}) - G(2.5_1)$, cal/mol	K , cal/(deg) ²
PLL PPII-	11	0.87	-74	2.7
PLL 2.5 ₁	11			2.6
PGA PPII	22	0.76	-152	1.0
PGA 2.5 ₁	5			4.9
PLL-PGA β -sheet	23	N/A	N/A	0.73

^a The table lists the standard deviation of the Ψ angle, σ , the ratio R of amplitudes of the 2.5₁-helix relative to that of the PPII conformation, the Gibbs free energy difference between the 2.5₁-helix and the PPII conformations, and the torsional constant K for Ψ angle deformations.

PGA and PLA samples contain a mixture of PPII and extended β -strand-like conformations.

Assuming similar Raman cross sections for these conformations, we roughly estimate that “unfolded” PLL and PGA both consist of ~60% PPII and ~40% β -strand. In contrast, we only detect very small contributions from β -strand-like conformations in AP at high temperature.³⁶ The lack of a temperature dependence of the relative intensity ratios suggests that these conformations have similar energies (Table 4).

It should be noted that Raman optical activity studies of “unfolded” peptides and proteins show positive features between ~1314 to ~1325 cm⁻¹, which are thought to signal the PPII conformation.^{93–96} The large frequency spread for these positive bands may indicate the existence of a variety of PPII-like left-handed helical conformations with significantly differing Ψ and Φ angles.

(94) Barron, L. D.; Blanch, E. W.; Hecht, L. *Adv. Prot. Chem.* **2002**, *62*, 51–90, 51 plates.

(95) Blanch, E. W.; McColl, I. H.; Hecht, L.; Nielsen, K.; Barron, L. D. *Vib. Spectrosc.* **2004**, *35*, 87–92.

(96) McColl, I. H.; Blanch, E. W.; Gill, A. C.; Rhie, A. G. O.; Ritchie, M. A.; Hecht, L.; Nielsen, K.; Barron, L. D. *J. Am. Chem. Soc.* **2003**, *125*, 10019–10026.

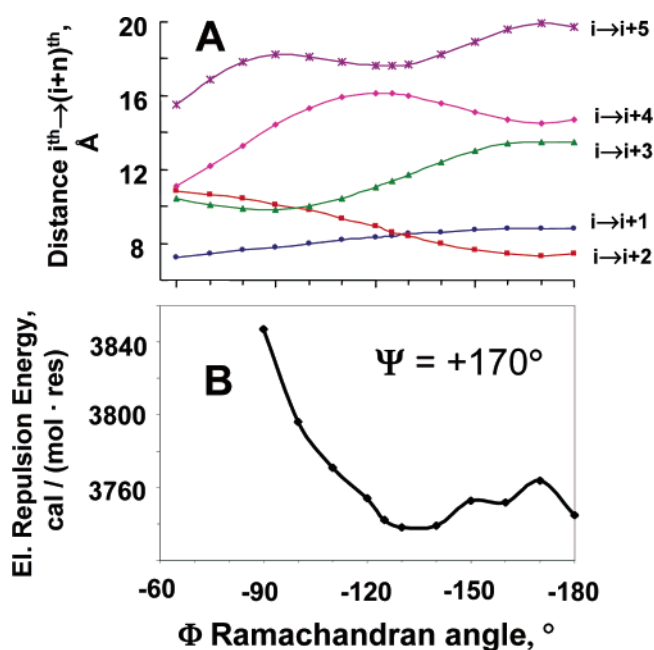


Figure 3. (A) Distances between the i -th and $(i+k)$ -th side chain charges of PGA as a function of the Φ Ramachandran angle as calculated using HyperChem. (B) Electrostatic repulsion energy between the side chains as a function of the Φ Ramachandran angle. NOTE: The Ψ angle is fixed at the value of 170° estimated from the UV Raman data.

Whatever the case, we detect only PPII and extended β -strand-like conformations that significantly differ spectrally from those of β -sheet conformations (compare Figures 2, 7, and 8).

As discussed below (eq 2), the ~1271 cm⁻¹ AmIII₃^S band frequency results in a calculated β -strand-like Ψ angle of ~170°, if we neglect any Φ angle frequency dependence. This neglect of the Φ angle dependence is justified in view of the known small Φ angle amide III frequency dependence^{60,67} and the fact that only modest changes in the Φ angle are likely to occur between the relevant conformations with different Ψ angles. Further, we and others recently estimated that the Ψ angle dependence can result in up to an ~110 cm⁻¹ shift,⁶¹ while the Φ angle results in no more than a 20 cm⁻¹ AmIII₃ frequency shift.^{67,68}

The β -Strand-like Conformation Is a 2.5₁-Helix. We developed insight into this new conformation by examining the dependence of the electrostatic repulsion energies on the Φ angle for a fixed Ψ angle of $+170^\circ$ (Figure 3). We utilized the HyperChem amino acid database to construct approximate structures to estimate the distances between charges located on PLL and PGA side chains. Figure 3 shows that the total

Extended 2.5₁-helix (left-handed):

$$\Psi = +170^\circ, \Phi = -130^\circ$$

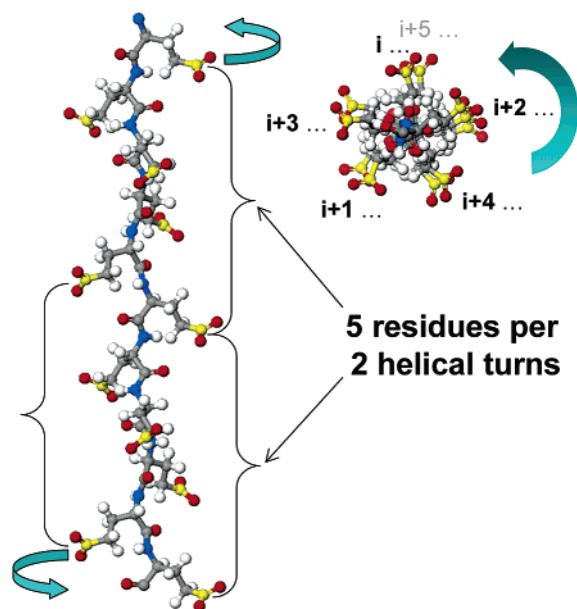


Figure 4. Visualization of the 2.5₁-helix in PGA ($\Psi = +170^\circ$, $\Phi = -130^\circ$). This structure occurs in both ionized PLL and PGA due to electrostatic repulsion between bulky and charged side chains. Carboxyl carbons of glutamic acid side chains are shown in yellow.

electrostatic repulsion energy has a minimum near $\Phi \approx -130^\circ$ for PGA. The situation for PLL has the same trend (Table 3).

Figure 4 indicates a rough structure for our PGA minimum repulsion energy conformation, which utilizes the determined Ψ and Φ angles of $+170^\circ$ and -130° , respectively. The resulting extended β -strand occurs as a 2.5₁-helix conformation.

Krimm and Mark's⁹⁷ previous theoretical study of conformations of polypeptides with ionized side chains also proposed that the charged side chains of PLL and PGA stabilize a helical conformation with approximately 2.5 residues per helical turn. They also showed that the number of residues per turn was essentially independent of side chain length for side chains equal to or longer than that of glutamic acid. However, for a 64-residue PGA they proposed a minimum energy conformation with $\Psi = -170^\circ$ and $\Phi = -155^\circ$ (in their original article they used an older definition for the Ψ and Φ angles).⁹⁸ Future work will be required to discriminate between these very similar structures to determine the actual Φ angles.

Our study here is the first, to our knowledge, to experimentally detect a stable 2.5₁-helix conformation in peptides and proteins. We also compared the distances between charges in our putative 2.5₁-helix to those in a PPII helix. Table 3 shows that the larger separation distances occur in the 2.5₁-helix compared to the PPII helix. This lowers the 2.5₁-helix total energy such that it is very close to that of the PPII conformation (Table 4).

Our spectral data and the lack of a significant temperature dependence of the relative Raman intensities clearly demonstrate

(97) Krimm, S.; Mark, J. E. *Proc. Natl. Acad. Sci. U.S.A.* **1968**, *60*, 1122–1129.

(98) Note that Krimm and Mark in their article (ref 97) used old Ψ - and Φ angle convention, since the modern one was not yet in effect. Thus, their $\psi = +10^\circ$ and $\Phi = +25^\circ$ correspond to -170° and -155° of the modern convention, respectively.

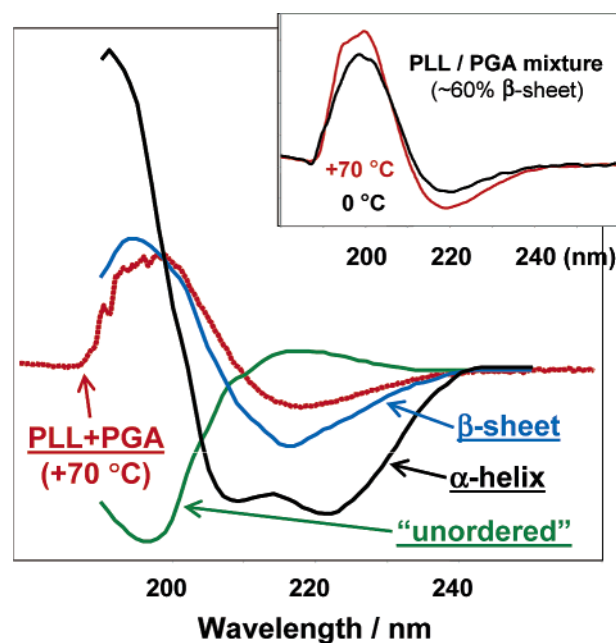


Figure 5. Comparison of CD spectra of different peptide and protein conformations to that of a neutral pH mixture of PLL and PGA at $+70^\circ\text{C}$. This sample obviously contains a significant fraction of β -sheet, due to the similarity of the PLL and PG mixture CD spectrum to that of the β -sheet. The pure secondary structure CD spectra were obtained from the Lawrence Livermore National Laboratory Web site (<http://www-structure.llnl.gov/cd/tutorial.htm>).

that these conformations are close in energy. Given our present inability to accurately curve resolve the PPII peak from the 2.5₁ AmIII₃ peaks, our incomplete understanding of the degeneracies of these two conformation, the unknown dependence of the Raman cross sections on conformation, and the measured modest temperature dependence, on the basis of the relative intensity ratios, we can only visually roughly estimate from the relative Raman intensities that the 2.5₁ conformations of PLL and PGA are <300 cal/mol higher in energy than the PPII conformation at room temperature (however, see below). We are in the process of modeling this 2.5₁-helix conformation to better determine its detailed geometry.

Our observations of the 2.5₁-helix was, in fact, partially presupposed by Tiffany and Krimm²² who originally proposed that aqueous solution denatured states of PLL and PGA would contain some local order and would not be in a completely “disordered” form. The structure was suggested to involve an extended 3₁-helix or a PPII helix, which is also a left-handed helix, with three amino acid residues per turn, with Φ - and Ψ -Ramachandran angles of -75° and 145° , respectively. In addition, more recent studies report evidence for PPII content in “unfolded” PLL and PGA.^{70–78,94–96}

2. PLL–PGA β -Sheet Conformation. Equimolar mixtures of PLL and PGA at neutral pH are known to form antiparallel β -sheets.⁵⁹ This is clearly demonstrated in the Figure 5 comparison of the CD spectrum of a PLL–PGA mixture to the CD spectra of α -helical, β -sheet, and “unordered” peptides. The PLL–PGA mixture spectrum, especially the ~ 217 -nm negative feature, clearly demonstrates a significant fraction of β -sheet. In addition, the CD spectra of the PLL–PGA mixture shows an increasing 217-nm trough as the temperature increases, which indicates that the β -sheet content slightly increases with temperature (see inset to Figure 5).

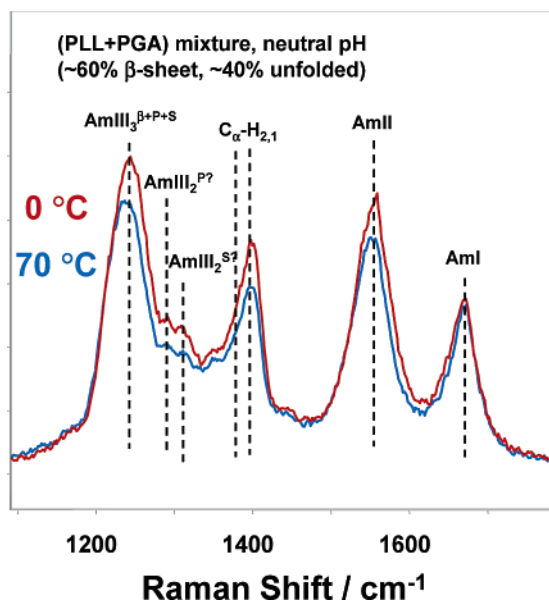


Figure 6. UVR spectra (204 nm) of neutral pH PLL–PGA mixture at 0 and +70 °C.

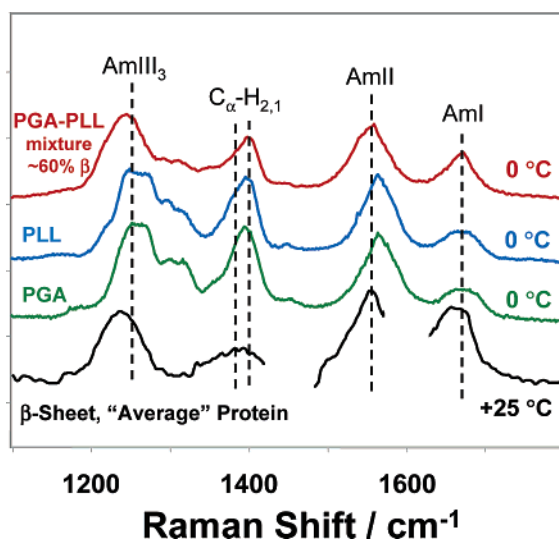


Figure 7. UVR spectra (204 nm) of PLL–PGA mixture at 0 °C, and those of the PPII and β -strand (2.5₁-helix) conformations of PLL and PGA. Also shown is the β -sheet basis spectrum determined by Chi et al.⁵² from a library of proteins.

Figure 6 shows the UVR spectra of the PLL–PGA mixture at 0 and +70 °C. The entire AmIII₃ band profile of the PLL–PGA mixture is red-shifted compared to unfolded PLL and PGA (Figures 1, 2, and 7, Tables 1 and 2) due to formation of the antiparallel β -sheet structure. Figure 6 shows that overall spectra of the PLL–PGA mixture are almost independent of temperature, indicating that the β -sheet conformation does not melt significantly over this temperature range. Further, the temperature dependence of the AmI, II, and III band frequencies in the PLL–PGA mixture ($\sim 60\%$ β -sheet) is significantly decreased (~ 2 -fold) compared to those in the PPII and β -strand (2.5₁-helix) conformations due to the decreased peptide–water hydrogen bonding of the β -sheet structure.

Calculation of Pure β -Sheet Spectrum from PLL–PGA Mixture UV Raman Spectra. The PLL–PGA mixture UVR spectra in Figures 6 and 7 are broad and show high frequency shoulders. This contrasts with the AmIII symmetric band shape

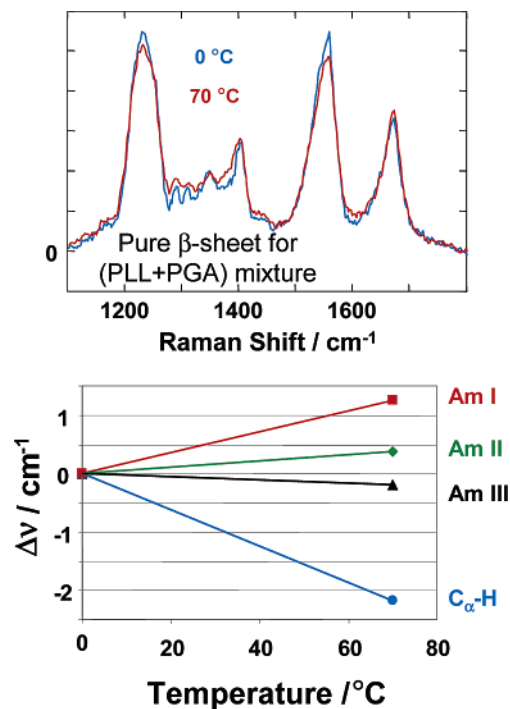


Figure 8. Calculated 204-nm UVRS of PLL–PGA mixture β -sheet spectrum at 0 and +70 °C. The contributions from the PLL and PGA PPII and β -strand (2.5₁-helix) conformations were numerically removed (see text for details). UVR bands of β -sheet show a very small temperature dependence compared to that of PPII (Table 2).

found by Chi et al.⁵² for the β -sheet conformation of a library of proteins (Figure 7). Thus, the PLL–PGA mixture sample appears to contain additional peptide conformations. Since the PLL and PGA side chains are highly ionized at this neutral pH, it is likely that these other conformations are the extended 2.5₁-helix and the PPII conformations discussed above.

We can calculate the pure β -sheet PGA–PLL Raman spectrum by subtracting off the spectra of these other conformations. We assume that the spectra of these other conformations are the sum of the individual PLL and PGA PPII and β -strand (2.5₁-helix) spectra. The criteria for the amounts subtracted are that the resultant spectra (Figure 7) best fit the β -sheet spectrum of Chi et al.⁵² (except that we do not include the amide I region in the fit due to the potential residual contribution of the water bending band). We find non- β -sheet conformation fractions of 42% at 0 °C and 35% at 70 °C. Thus, the β -sheet content slightly increases with temperature.

Figure 8 shows these calculated pure β -sheet spectra at 0 and 70 °C. The β -sheet AmIII peak is symmetric without any shoulders and is similar to that found by Chi et al.⁵² (compare Figures 7 and 8). As also shown in Figure 8, the pure PLL–PGA mixture β -sheet spectrum shows a ~ 10 -fold decreased temperature frequency dependence for the AmII and III bands and a ~ 3 -fold decreased AmI band frequency dependence than occurs for the PPII and 2.5₁-helix conformations. This is expected due to the decreased water–amide bond hydrogen bonding of the β -sheet since the β -sheet satisfies its hydrogen bonding mainly through interpeptide hydrogen bonds.

The large UVRS spectral differences between the PLL–PGA mixture pure β -sheet conformation and that of PLL and PGA in their unfolded states (compare Figures 8 and 7) offer opportunities for characterizing subtle issues of β -sheet con-

formation. This could be valuable in kinetic and steady-state investigations of systems such as amyloid fibrils.⁶²

Ψ Ramachandran Angular Distribution for PLL and PGA β -Sheet, PPII, and 2.5₁-Helix. The β -sheet, PPII, and 2.5₁-helix amide bands are significantly broadened from their estimated 7.5 cm⁻¹ homogeneous line width determined in crystals.³⁴ This broadening probably results from the distribution of Ψ angles that occurs for these conformations in solution. We developed a deconvolution method for the AmIII₃ band frequencies that determines the inhomogeneous distribution of AmIII₃ band frequencies.³⁴ We then developed a method to use this frequency distribution to calculate the Ψ angle distribution from the measured AmIII₃ band shapes.^{34,61} Originally³⁴ we utilized the following equation:

$$v_{\text{III3}}(\Psi) = 1265 \text{ cm}^{-1} - 46.8 \text{ cm}^{-1} \sin(\Psi + 5.2^\circ) \quad (1)$$

which allows us to roughly estimate the relationship between the AmIII₃ frequency and Ψ Ramachandran angle for peptides and proteins in water solutions. The sinusoidal nature of eq 1 was theoretically predicted by Asher et al.⁶⁰ and explained in terms of different degree of coupling between the N–H and C α –H bending motions at different Ψ angles.

In our most recent study,⁶¹ we examined the dependence of the AmIII₃ frequencies of peptide bonds upon the peptide bond hydrogen bonding. This study also elucidated the temperature dependence of the AmIII₃ frequencies that result from the temperature dependence of its hydrogen bonding. We quantified this hydrogen bonding-induced frequency dependencies for all major peptide/protein secondary structure conformations⁶¹ and were able to propose a family of equations to relate the AmIII₃ frequency directly to the Ψ Ramachandran angle given its particular state of hydrogen bonding.

Thus, for the peptide bonds of extended and highly exposed to water conformations, such as PPII and 2.5₁-helix, we would use eq 2:⁶¹

$$v_{\text{III3}}^{\text{EXT}}(\psi, T, \text{HB}) = [1256 \text{ cm}^{-1} - 54 \text{ cm}^{-1} \cdot \sin(\psi + 26^\circ)] - 0.11 \cdot \frac{\text{cm}^{-1}}{^\circ\text{C}} \cdot (T - T_0) \quad (2)$$

where $T_0 = 0$ °C.

In contrast, for PLL–PGA mixture antiparallel β -sheet, which is dominated by two end-on peptide bond–peptide bond hydrogen bonding,⁶¹ we would use eq 3:

$$v_{\text{III3}}^{i\alpha, i\beta}(\psi, T_0, \text{HB}) = [1244 \text{ cm}^{-1} - 54 \text{ cm}^{-1} \cdot \sin(\psi + 26^\circ)] \quad (3)$$

Figure 9 shows the Ψ angle distribution calculated for PLL (pH = 2) and PGA (pH = 9) and for the PLL–PGA mixture β -sheet. Figure 9 displays the existence of the two different conformations of unfolded PLL and PGA, with two distinct maxima near $\Psi \approx 145^\circ$ (PPII) and $\Psi \approx 170^\circ$ (2.5₁-helix).

As shown in Figure 9, these calculated distributions are well fit by Gaussian line shapes. The estimated standard deviation for PLL at pH = 2 is $\sigma \approx 11^\circ$ for both the PPII and the 2.5₁-helix conformations, while PGA at pH = 9 shows a broader distribution for PPII with $\sigma \approx 22^\circ$ and a sharper distribution for the 2.5₁-helix with $\sigma \approx 5^\circ$ (Table 4). Both of these distributions are consistent with an electrostatic repulsive

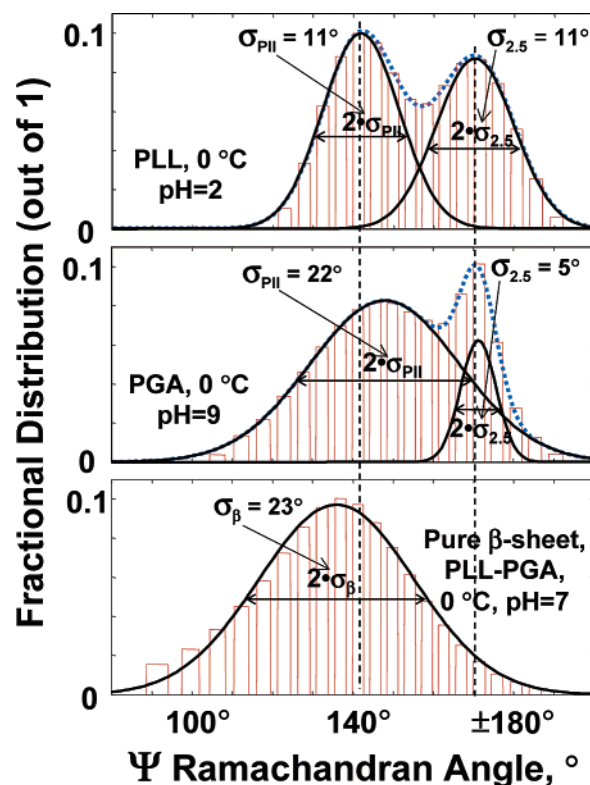


Figure 9. Estimated Ψ Ramachandran angular distribution for pH = 2 PLL and pH = 9 PGA samples and for the pure β -sheet conformation of the PLL–PGA mixture. The pure β -sheet spectrum was calculated by numerically removing the unfolded state contribution as discussed in the text.

interaction that destabilizes the PPII conformation relative to the 2.5₁-helix. The electrostatic interactions are larger for the shorter side chain PGA relative to PLL, which should lead to a sharper distribution of angles for the 2.5₁-helix. In fact, the PGA PPII conformation minimum Ψ angle is shifted toward that of the 2.5₁-helix conformation.

The calculated β -sheet spectrum of the PLL–PGA mixture shows the broadest distribution of Ψ angles with $\sigma \approx 23^\circ$. This indicates that the β -sheet conformations show the smallest energy penalty for changes in their Ψ angles. This is expected since a significant flexibility should exist for interpeptide bond hydrogen bond linkages; the angular dependence of hydrogen bond energies should be small around the equilibrium configuration.

Determination of Gibbs Free Energy Landscape for PPII \leftrightarrow 2.5₁-Helix along the Ψ Angle Reaction Coordinate. We can estimate the Gibbs free energy landscape of the PPII and 2.5₁-helix conformations along the Ψ angle reaction coordinate from the calculated Ψ angle distributions. We assume that the distributions have identical degeneracies and that the probability of each conformation to occur at a particular Ψ angle is given by a simple Boltzmann distribution:

$$\frac{n(\psi_i)}{n(\psi_o)} = \exp\{-[G(\psi_i) - G(\psi_o)]/N_A k_B T\} \quad (4)$$

where $n(\Psi_i)/n(\Psi_o)$ is the ratio of populations with Ramachandran angles Ψ_i and Ψ_o , $G(\Psi_i)$ is the Gibbs free energy of the conformation with angle Ψ_i , $G(\Psi_o)$ is the Gibbs free energy at

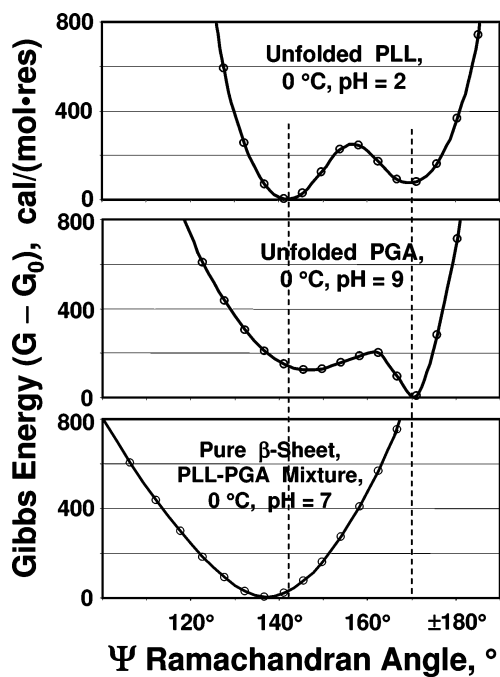


Figure 10. Estimated Gibbs free energy landscapes $G - G_0$ for pH = 2 PLL, pH = 9 PGA, and PLL–PGA pure β -sheet along the Ψ angle coordinate. We define $G_0 = G(\Psi_0) = 0$ (see text for details).

the lowest conformational energy, N_A is Avogadro's number, k_B is the Boltzmann constant, and T is temperature.

Thus, the Gibbs free energy difference between the PPII and 2.5₁-helix conformations can be estimated as:

$$\Delta G = G_{\text{PPII}} - G_{2.5_1} = -N_A k_B T \ln(n_{\text{PPII}}/n_{2.5_1}) = -N_A k_B T \ln R \quad (5)$$

where R is the fractional distribution ratio at the energy minimum of the two conformations in Figure 9.

Using eq 5, we obtain ΔG values of -152 and -74 cal/mol for PGA and PLL, respectively, for Ψ angles at the minimum of these energy distributions (see Table 4). The fact that these Ψ angle distributions are well modeled by Gaussians (Figure 9) results from the fact that the potential energy of a conformation about its equilibrium is given by $E = E_0 + K\Delta\Psi^2$, where E_0 is the energy at the minimum Ψ of a conformation and K is the torsional force constant. Table 4 shows that the torsional constant is the smallest for the β -sheet conformation while it is the largest for the PGA 2.5₁ conformation. The 2.5₁-helix \rightarrow PPII crossing barriers for PLL and PGA have similar values of ~ 170 and ~ 200 cal/mol, respectively. In contrast, PPII \rightarrow 2.5₁-helix crossing barriers for PLL and PGA have values of ~ 250 and ~ 70 cal/mol, respectively. These observations are expected, since the stronger electrostatic repulsion between charges located on shorter side chains of PGA (with respect to that of PLL) should stabilize the 2.5₁-helix and destabilize the PPII conformations.

We can use this information to calculate the Gibbs free energy landscape of these peptides along the Ramachandran Ψ angle coordinate (Figure 10). We do not know the absolute energy scale to relate the energy landscapes of these different peptides. However, shown here are the relative Gibbs energies, $G - G_0$. For each peptide, we assign the Gibbs energy value at the lowest conformational energy G_0 to be zero. We find similar energy

landscapes for PGA and PLL when their side chains are ionized. The side chain electrostatic repulsions lower the 2.5₁-helix conformation energy relative to that of the PPII conformation. This effect is more significant for the shorter side chain PGA peptides, where the electrostatic repulsions exert a larger energetic penalty for deviations from the minimum energy Ψ angle conformation geometry of the 2.5₁-helix. The barriers between these two conformations are slightly less than $N_A k_B T$ (~ 540 cal/mol at 0 °C). Thus, it is likely in solution that these conformations rapidly interconvert. The major changes in geometry would involve mainly the Ψ and Φ coordinates. These changes would merely change the number of residues per turn.

The α -helix conformation is the most stable PGA and PLL conformation at 0 °C if the side chains are neutralized by changing pH.^{60,99} In this case, the α -helix conformations melt mainly to the PPII conformations upon temperature increases to room temperature.

The molecular mechanism of this conformational change is difficult to envision since not only do the interpeptide hydrogen bonds have to rupture, but the helix must also unwind and then rewind to reverse its handedness. Previous considerations of α -helix melting imagined that it was induced by the stepwise α -helix hydration which stabilized intermediates such as β -turns and reverse turns.^{100–102} However, the set of steps that would lead to a reverse helix are harder to visualize.

Conclusions

Our study of unfolded states of PLL and PGA indicates that they exist as a mixture of PPII and the extended 2.5₁-helix (β -strand-like) conformations. The charged side chains of pH = 2 PLL and pH = 9 PGA force the PLL and PGA chains in water to adopt more extended conformations to minimize interchain repulsions. The β -sheet structure of the PLL–PGA mixture showed little evidence for hydrogen bonding between the polypeptide backbone and water. We also utilized a new algorithm that allowed us to estimate the Ψ Ramachandran angle from the AmIII₃ frequency. This analysis demonstrates that each conformation has a distribution of Ψ angles about the minimum Ψ conformational energy. The Ψ angle distribution of the PGA 2.5₁-helix, which is sharper than that of PLL 2.5₁-helix, as well as the absence of the 2.5₁-helix conformation in alanine-based peptides are consistent with the hypothesized electrostatic mechanism of stabilization of the 2.5₁-helix. We were able to calculate the Ψ angle energy landscape of these observed conformations. This is an important advance since the Ψ angle coordinate is the most important coordinate for protein and peptide secondary structure changes.

Acknowledgment. We thank the NIH (Grant 8 RO1 EB002053021) for financial support.

JA044636S

- (99) Song, S.; Asher, S. A. *J. Am. Chem. Soc.* **1989**, *111*, 4295–4305.
 (100) Sundaralingam, M.; Sekharudu, Y. C. *Science* **1989**, *244*, 1333–1337.
 (101) Blanch, E. W.; Morozova-Roche, L. A.; Cochran, D. A. E.; Doig, A. J.; Hecht, L.; Barron, L. D. *J. Mol. Biol.* **2000**, *301*, 553–563.
 (102) McColl, I. H.; Blanch, E. W.; Hecht, L.; Barron, L. D. *J. Am. Chem. Soc.* **2004**, *126*, 8181–8188.